International Journal of Peptide Research and Therapeutics
https://doi.org/10.1007/s10989-019-10004-7

SHORT COMMUNICATION

Phosphinic Dehydrodipeptides: Diversification of the P1′ Residue with the Morita–Baylis–Hillman Acetates and Inhibition of Alanyl Aminopeptidases

Michał Talma[1]

Received: 4 November 2019 / Revised: 16 December 2019

Abstract
Activated allyl acetates (the Morita–Baylis–Hillman acetates) were confirmed as convenient electrophilic precursors of the P1′ fragment of phosphinic dehydrodipeptides, and then, their selected saturated analogs were obtained in the subsequent reduction. This approach is particularly appropriate for structurally complex side chains and thus is an alternative to the addition of α-substituted acrylates with aminoalkylphosphinic acids. While phosphinic dehydrodipeptides were found to be good inhibitors of two mammalian alanyl metalloaminopeptidases, the saturated compounds showed higher activities than their structurally constrained counterparts. Docking calculations and molecular modeling showed that conformational freedom allowed for the favorable binding of distinct stereoisomers of phosphinates, while the presence of the double bond was more restrictive.

Keywords Morita–Baylis–Hillman reaction · Nucleophilic substitution · Phosphinic peptide analogs · Enzyme inhibitors · Mammalian alanyl aminopeptidase

Introduction

Phosphinic acid peptide analogs are well-recognized transition-state analog inhibitors of metal-dependent hydrolases, particularly the medically significant proteases (Collinsová and Jirácek 2000; Georgiadis and Dive 2015; Mucha et al. 2011; Yiotakis et al. 2004). The competitive and reversible mechanism of their action involves the coordination of the tetrahedral phosphinic function with catalytic metal ion(s) and specific interactions of pseudopeptide side-chain residues with the corresponding binding pockets of an enzymatic target (Mucha et al. 2011; Yiotakis et al. 2004). The structural complementarity is of particular importance for the dipeptidyl analog inhibitors that basically explore the S1 and S1′ cavities that are the clefts closest to the reaction site. Careful structural refinement of the corresponding P1 and P1′ substituents, which frequently leads to non-proteinogenic side chains, was shown to provide highly potent dipeptide-mimicking ligands (Mucha 2012). The most remarkable examples involve action on zinc-containing aminopeptidases as demonstrated by the inhibition of the members of M01 and M17 exopeptidase families that are multifunctional broad-band specificity enzymes involved in biological functions in eukaryotic and prokaryotic cells; their deregulated activity is associated with human diseases such as cancer, and they are also etiological factors in protozoal and bacterial infections (Chen et al. 2000; Skinner-Adams et al. 2010; Suzuki et al. 2004; Vassliou et al. 2014; Wang et al. 2007). Synthetic preparation of phosphinic dipeptides is achieved either by a phospha-Michael addition of a silylated N-protected aminoalkyl-*H*-phosphinic acid to an α-substituted acrylate (Thottathil et al. 1984) or by a three-component amidoalkylation reaction (Chen and Coward 1996). The fundamental starting materials for these extensively explored reactions are aldehydes that are precursors of the P1 residue (Baylis et al. 1984) and acrylates that code the P1' fragment (Boyd et al. 1990; Stetter and Kuhlmann 1979). As the side chains must ensure tight ligand-protein interactions, they frequently demand modifications with heteroatom-containing functional groups. These additional modifications require the development of complex multistep synthetic pathways

✉ Michał Talma
michal.talma@pwr.edu.pl

[1] Department of Bioorganic Chemistry, Faculty of Chemistry, Wrocław University of Science and Technology, Wybrzeże Wyspiańskiego 27, 50-370 Wrocław, Poland

Published online: 02 January 2020

and an orthogonal protection strategy and are particularly challenging for the diversification of α-substituted acrylates (Mucha 2012).

Activated allyl acetates (Morita–Baylis–Hillman acetates) are synthetically feasible but rarely reported precursors of the P1′ substituents in phosphinic pseudodipeptides. The allyl acetates are products of acetylation of allyl alcohols that are universally obtained in the Morita–Baylis–Hillman reaction of aldehydes with alkyl acrylates (Morita et al. 1958). Such adducts are capable of an S_N2' displacement reaction with phosphorus nucleophiles (Kalyva et al. 2015; Talma and Mucha 2017), including silylated N-protected aminoalkyl-*H*-phosphinic acid to provide P1′-dehydro-modified dipeptide analogs (Scheme 1, pathway A) (Matziari et al. 2001).

The synthesis and biological activity of phosphinic dehydrodipeptides are much less recognized than their saturated counterparts. Regarding the synthesis, in an alternative to the abovementioned MBH adducts-based approach (Kalyva et al. 2015; Matziari et al. 2001; Talma and Mucha 2017), P1′-α,β-unsaturated phosphinic dipeptides may be obtained from active methylene compounds. Additions of trialkyl phosphonoacrylates or dialkyl methylidenemalonates to H-phosphinic acids were reported to provide phosphinate-substituted phosphonoacetates or malonates, respectively, that could subsequently undergo either Wittig-Horner olefination (Parsons et al. 1988) or Knoevenagel-type condensation (Gurulingappa et al. 2003; Matziari et al. 2006) (Scheme 1, pathway B). The unsaturated products have usually been considered as intermediates for further transformations. These transformations mainly involved the catalytic hydrogenation of the double bond that is conveniently performed in a stereoselective manner, thus leading to phosphinic dipeptides with the desired P1′ stereochemistry (Georgiadis et al. 2004; Parsons et al. 1988; Yamagishi et al. 2011). Accordingly, D-Alaψ[P(O)(OH)CH_2]-D-Ala (the phosphinic acid analog of D-Ala-D-Ala dipeptide) was obtained and used to study the inhibition of the D-Ala-D-Ala ligase, a bacterial enzyme involved in cell wall biosynthesis (Parsons et al. 1988). The α,β-conjugated system of P1'-dehydroalanine synthons was also utilized as the Michael acceptors to add nitrogen, carbon and sulfur nucleophiles (Matziari et al. 2001; Matziari et al. 2004). The reactions proceeded under mild conditions and without the protection of the phosphinate moiety. The diversification potential was implemented to construct potent and selective inhibitors of matrix metalloproteases, particularly MMP-11 (Matziari et al. 2004). Inhibition of renal dipeptidase is probably the only reported example of direct biological application of phosphinic P1'-dehydrodipeptides (Gurulingappa et al. 2003; Gurulingappa et al. 2004; Parsons et al. 1991). The compound bearing hydrophobic side-chain residues showed a high affinity against the enzyme (IC_{50} of a low nanomolar value), with a preference for the *Z* configuration (stereoisomers separated chromatographically) (Gurulingappa et al. 2004).

In this work, we report the synthesis and activity of phosphinic dehydrodipeptides as inhibitors of mammalian alanyl aminopeptidases. Bulky aromatic residues, including those substituted with functionalities, were introduced as the rigid P1' portion of the molecules. The preparation protocol was based on the Morita–Baylis–Hillman acetates as versatile and diversified precursors. The impact of the P1' constraints

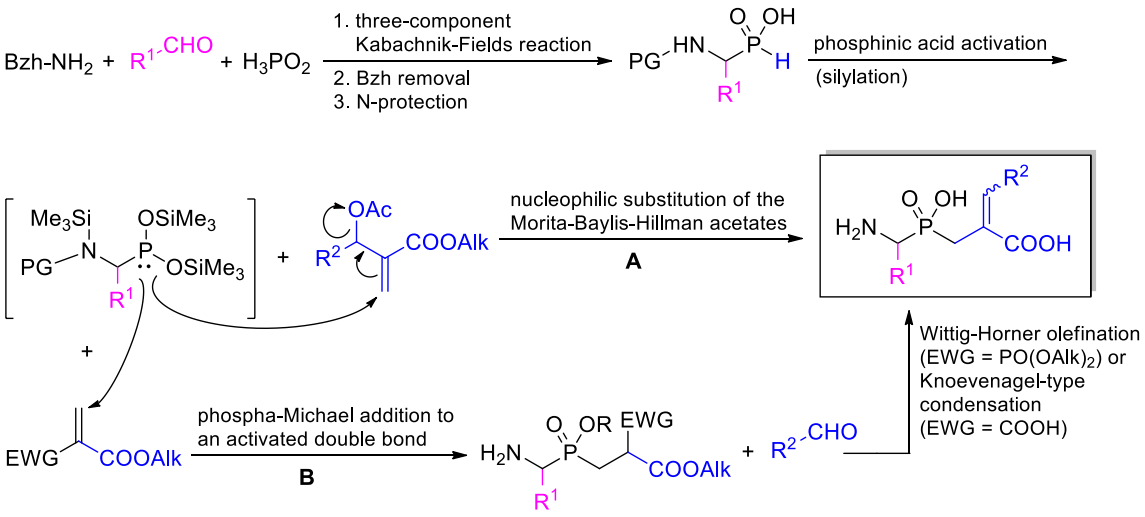

Scheme 1 General reaction scheme of the synthetic pathways leading to dehydrodipeptides.

on the biological activity was assessed in relation to the potency of the selected saturated analogs.

Materials and Methods

General

All used reagents, solvents, aminopeptidases (recombinant human and microsomal porcine kidney APNs, the lyophilized forms) and the fluorogenic substrate (L-alanine-4-methylcoumaryl-7-amide) were purchased from commercial suppliers. Dry toluene was obtained by distillation over P_2O_5. Dry THF was obtained by distillation with sodium with benzophenone. Reactions were monitored by thin-layer chromatography carried out on 0.25 mm silica gel plates (silica gel 60F254) and components were visualized by UV light absorbance. Purification of compounds by flash chromatography was carried out on the CombiFlash® Rf^+ Lumen chromatographic system with the use of prepacked silica or C18 columns. ^1H, ^{13}C and ^{31}P NMR spectra were recorded on Bruker Avance DRX 600 MHz and JEOL JNM-ECZ 400S Research FT NMR spectrometers. HRMS spectra were recorded on a Waters ESI-Q-TOF Premier XE mass spectrometer. All synthesized compounds gave satisfactory NMR and HRMS spectra. Analytical HPLC was performed on UltiMate 3000 LC System (Dionex) using H_2O/ACN elution system (0%, 5 min, then, 0% → 100%, 20 min). Inhibition constants were calculated from the spectrofluorometric measurements carried out on Spectra MAX Gemini EM fluorimeter.

Synthesis of Phosphinic Dehydrodipeptides (Vassiliou et al 1999; Grembecka et al. 2003)

In an oven-dried three-necked flask, 1-(*N*-benzyloxycarbonylamino)-3-phenylpropyl-*H*-phosphinic acid **3** (1.00 g, 3 mmol) (Baylis et al. 1984; Grembecka et al. 2003) and hexamethyldisilazane (10–15 mL) were heated at 90–110 °C for 2–3 h under Ar. Then, the reaction mixture was cooled to room temperature and the appropriate MBH acetate **2** (Basavaiah and Pandiaraju 1996; Yu et al. 2001) (4.20 mmol, 1.4 eq.) dissolved in toluene (5 mL) was added. The mixture was heated again at 90–110 °C for 2–3 h, then, cooled to room temperature. MeOH (5 mL) was added and the mixture was stirred overnight. The volatiles were evaporated in vacuo and the residue was partitioned between ethyl acetate and 5% $KHSO_4$ (50 mL:50 mL) for extraction. The water phase was discarded and the organic phase was washed again with 5% $KHSO_4$ and brine (50 mL of each). The organic phase was dried over Na_2SO_4, evaporated in vacuo and the residue was purified by flash chromatography on silica using *n*-hexane/AcOEt (0% → 100%) → AcOEt/MeOH (0% → 100%) elution system to yield **4.**

Protective Group Removal—Representative Examples 4e and 4h

The biphenyl derivative of amino- and carboxylate-protected phosphinic dehydrodipeptide **4e** (0.3 g, 0.5 mmol) was stirred with 33% solution of HBr in acetic acid (5 mL) for 1–2 h, then, the volatiles were evaporated in vacuo. The residue was dissolved in MeOH (20 mL) and propylene oxide (2 mL) was added to quench the remaining HBr. The following addition of cold diethyl ether (10 mL) precipitated the crude product. The solid was separated by centrifugation and solvent decantation. The crude peptide **5e** was purified by flash chromatography on a C18 reversed phase column in H_2O/acetonitrile (0 → 100%) eluent.

The mesyl derivative of amino- and carboxylate-protected phosphinic dehydrodipeptide **4h** (0.322 g, 0.5 mmol) was stirred with trifluoroacetic acid (10 mL) in the presence of thioanisole (1 mL) for 24 h at room temperature, then, the volatiles were evaporated *in vacuo*. The following addition of cold diethyl ether (10 mL) precipitated the crude product. The solid was separated by centrifugation and solvent decantation. The crude peptide **5h** was purified by flash chromatography on a C18 reversed phase column in H_2O/acetonitrile (0 → 100%) eluent.

Double Bond Reduction (Kalyva et al. 2015; Georgiadis et al. 2003)

Nickel(II) chloride (0.323 g, 2.50 mmol, 10 eq.) was added to a protected phosphinic dehydrodipeptide **5e** or **5h** (0.25 mmol) dissolved in the mixture of dry THF (10 mL) and absolute EtOH (5 mL), and cooled to - 30–40 °C. Sodium borohydride was added (0.189 g, 5.00 mmol, 20 eq.) in three portions and the reaction was stirred for 1 h, then, evaporated in vacuo. The residue was partitioned between ethyl acetate and 5% $KHSO_4$ (25 mL:25 mL) for extraction. The water phase was discarded and the organic phase was washed again with 5% $KHSO_4$ and brine (two times, 25 mL of each). The organic phase was dried over Na_2SO_4, evaporated in vacuo and the residue was purified by flash chromatography on silica using AcOEt/MeOH (0% → 100%) eluent. The removal of the protection groups was achieved as described above for unsaturated derivatives.

Molecular Modeling

Molecular modeling studies were performed using the Biovia Discovery Studio package and the GOLD package. The crystal structure of the enzymes *Hs*APN (PDF:4FYT)

(Wang et al. 2007) and *Ss*APN (PDB:6BV0) (Joshi et al. 2017) were used. The ligands and waters were removed and appropriate protonation states in the relation to experimental studies were established: 7.0 pH for *Hs*APN and 7.5 pH for *Ss*APN. Ligands were protonated as well and optimized with the use of CHARMm force field and Smart Minimizer algorithm, up to 0.1 Å. The docking sites were determined from the cavity option and the sphere representation limited to the 11 Å (*Hs*APN) and 15 Å (*Ss*APN) radius from the point of the metal ion in the active center. Molecular docking studies were performed by consecutive application of GOLD and In-Situ Minimization using Smart Minimize algorithms. The GOLD program is implemented in BIOVIA DS. GA parameters were changed to Automatic Very Flexible. Smart Minimizer algorithm optimized the results with all the other protein residues outside the docking sphere kept fixed. The binding energy of all docking poses were calculated according to the equation:

$$\Delta G_{\text{Binding\_energy}} = \Delta G_{\text{Complex\_energy}} - \Delta G_{\text{Protein\_energy}} - \Delta G_{\text{Ligand\_energy}}$$

Enzyme Inhibition Assays (Vassiliou et al. 2014)

A 96-well plate format was used in spectrofluorometric measurements. The excitation wavelength was set on 355 nm while the emission wavelength at 460 nm. Enzymes were preincubated for 30 min at 37 °C. The release of the AMC fluorophore was measured continuously for 45 minutes. The velocity was calculated from the linear part of the progress curve. The competitive version of Cheng–Prusoff equation allowed to compute the K_i values: $K_i = IC_{50}/[1 + (S/K_m)]$. Concentration of the inhibitor equal to 50% inhibition was shown as IC_{50} value calculated from relation of the hydrolysis velocity to the logarithm of the inhibitor concentration [I]. The SoftMax Pro, GraphPad Prism and Microsoft Excel programs were used for kinetic parameters calculations.

Results and Discussion

Activated allyl acetates **2a–h**, the electrophilic starting materials for obtaining the target dehydrodipeptides, were synthesized in a typical two-step procedure that involved the Morita–Baylis–Hillman reaction of aldehydes with an acrylate, followed by acetylation (Basavaiah and Pandiaraju 1996; Yu et al. 2001) (Scheme 2). Phenylalkyl aldehydes and *p*-substituted benzaldehydes **1a–h** were selected to deliver bulky aromatic P1' side chains. The hydroxy group of **1h** was mesylated. N-Cbz protected α-aminoalkyl-*H*-phosphinic acid **3**, the analog of homophenylalanine (Baylis et al. 1984; Grembecka et al. 2003), was used as the conserved nucleophilic component. The phenylethyl side chain of this substrate is known to be favorably bound in the corresponding S1 pocket of several M01 and M17 metalloaminopeptidases (Grembecka et al. 2003; Mucha 2005; Mucha et al. 2011; Vassiliou et al. 2014). The displacement reaction proceeded gently under the activation of the H-phosphinic acid to its tervalent ester with hexamethyldisilazane (Scheme 2). The crude products **4a–h** were separated after methanolysis and were purified chromatographically to provide either an *E*/*Z* diastereomeric mixture (not separated) or pure *Z* stereoisomers. Deprotection in acidic conditions gave the final compounds **5a–h**. The cleavage of the mesyl group from the phenolic -OH group of **5h** was achieved using ammonium hydroxide to yield **5i** (Ohgiya and Nishiyama 2004).

The phosphinic dehydrodipeptides were tested for inhibition of two mammalian M01 metalloaminopeptidases, namely, porcine and human alanyl aminopeptidases (APNs). The dipeptidyl analogs appeared to be potent, competitive and fast-binding compounds with inhibitory constants, K_i, in the low micromolar range for porcine kidney (*Ss*APN) and with submicromolar values for the human ortholog (*Hs*APN, Table 1). Expanded, hydrophobic and heteroatom-free substituents (benzyl, styryl and biphenyl) of the P1' double bond (compounds **2b**, **2d** and **2e**, respectively) gave rise to the most significant inhibition (K_i = 0.85–2.88 μM for *Ss*APN and K_i = 0.134–0.151 μM for *Hs*APN). The high affinity of the biphenyl-based P1' residue to the APNs was previously reported for phosphinic tripeptide analogs (Chen et al. 2000). Dehydropeptides **5g** and **5i** containing the phenyl group functionalized with nitro and hydroxy groups also displayed very good affinity, particularly for the human aminopeptidase (K_i = 0.192 μM and K_i = 0.18 μM, respectively).

Although the anti-aminopeptidase activity of phosphinic dehydrodipeptides was found to be satisfactory, it did not achieve the excellent nanomolar level reported previously for saturated analogs (Grembecka et al. 2003; Vassiliou et al. 2014). For example, hPheψ[P(O)(OH)CH_2]-Phe inhibited *Hs*APN with K_i = 0.002 μM (Vassiliou et al. 2014) (K_i = 0.62 μM for the corresponding dehydro derivative **5a** reported here) while hPheψ[P(O)(OH)CH_2]-Tyr inhibited *Ss*APN with K_i = 0.036 μM (Grembecka et al. 2003). (K_i = 3.82 μM for the corresponding **5i**). Apparently, the double bond constraints led to a decrease in the potency by more than two orders of magnitude. To further illustrate this result, we reduced two phosphinic dehydrodipeptides (**5e** and **5 h**) to their saturated analogs (**6e** and **6h**) and compared their activities. The reduction proceeded readily with the use of sodium borohydride in the presence of nickel chloride at low temperature as described elsewhere (Kalyva et al. 2015; Georgiadis et al. 2004). Indeed, the saturated phosphinic peptides inhibited the tested metalloaminopeptidases much more effectively than the dehydropeptides (Table 2). Only the potency of **6e**

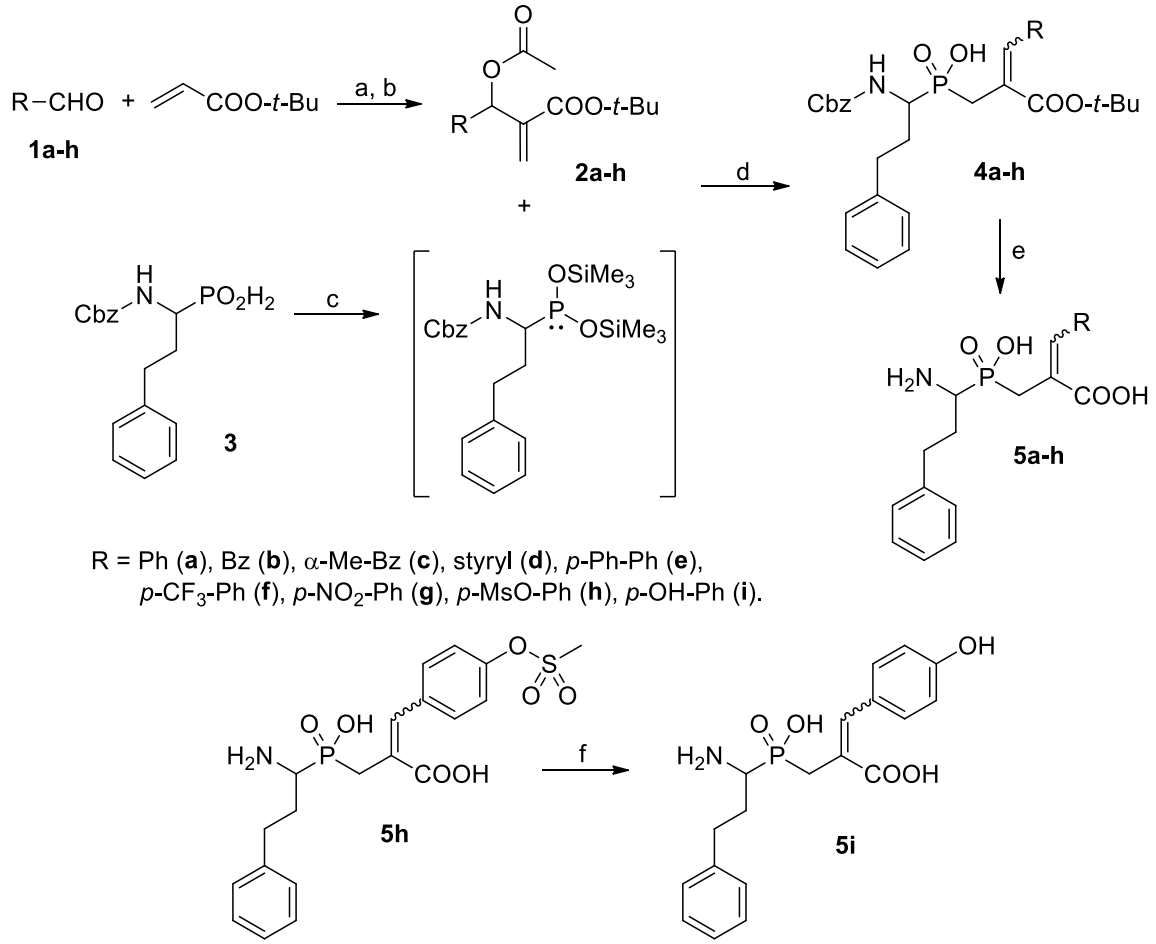

Scheme 2 Synthesis of phosphinic dehydrodipeptides from the Morita–Baylis–Hillman acetates as the P1' precursors. Reagents and conditions: **a** DABCO, DMSO/H_2O, rt, 7 days; **b** AcCl, Et_3N, dry CH_2H_2, 0 °C, 1 h, rt, 16–24 h; **c** HMDS, 95–110 °C, Ar, 2 h; **d 2a–h** in dry toluene, 90–115 °C, Ar, 2–3 h, then MeOH, rt, 16–24 h; **e** 33% HBr in AcOH, rt, 2 h or TFA, thioanisole, rt, 24 h (for **4 h**); **f** 25% $Me_4N^+OH^-$ in H_2O, MeOH, 10 Eq. rt, 24 h.

against *Ss*APN remained at the same level as the potency of **5e**. In the other cases, reduced compounds improved the affinity toward APNs by a factor of 7–28. K_i values for human APN were below 0.035 μM, with the biphenyl-substituted analog being the most active found in this study ($K_i = 0.021$ μM).

To obtain an additional insight into the structure-activity relationship, we performed docking simulations for P1'-unsaturated and saturated dipeptides using the GOLD docking protocols with *in situ* minimization and calculated the free binding energies. Although the compounds were assayed for kinetics with APNs as the mixtures, the calculation protocols were performed for individual stereoisomers, taking into account the *R*/*S* and *E*/*Z* configurations (Table 2). Considering the best poses, compounds **6e** and **6h** were energetically more favorable to some extent than **5e** and **5h**. Due to their rotational freedom, the latter-mentioned inhibitors could more easily balance the positioning of the phosphinic group against the zinc ion, with the simultaneous penetration of the corresponding binding pockets with the P1 and P1' side chains.

Clearly, the binding is not optimal for each stereoisomer, as indicated by the detailed correlations of the energies with the configurations. Among the unsaturated compounds, with a single exception, *Z* geometrical isomers appeared disadvantageous and lost the opportunity for canonical binding with the zinc ion (Table 2). As *Z* stereochemistry is dominant for the synthesized samples, such an unfavorable composition could be the reason for their lower than expected potency. The exception was the biphenyl derivative **5e** bound to *Hs*APN, and all four diastereoisomers were characterized by high binding energy values. Among these, only the *R*-(*E*) form was an exception to the standard mode of action. Accordingly, **5e** was one of the most potent compounds against *Hs*APN among the dehydrodipeptides. In this case, the advantageous overall conformations of the stereoisomers are driven by the complementarity of the biphenyl to the large hydrophobic pocket.

Table 1 Inhibition of porcine (*Sus scrofa*, *Ss*) and human (*Homo sapiens*, *Hs*) alanyl aminopeptidase (APN) by phosphinic dehydrodipeptides **5a–i** bearing aromatic substitution of the P1' double bond

Entry	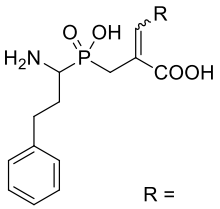 R =	Inhibition, K_i [μM]	
		*Ss*APN	*Hs*APN
5a		36.8±1.2	0.620±0.20
5b	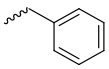	2.88±0.83	**0.151±0.031**
5c	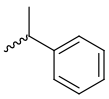	6.85±2.6	0.254±0.060
5d	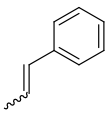	1.92±0.15	**0.134±0.023**
5e	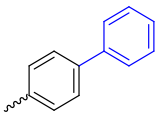	0.850±0.060	**0.151±0.028**
5f	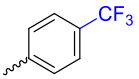	13.0±5.1	0.491±0.086
5g	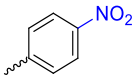	9.70±0.28	**0.192±0.018**
5h	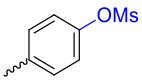	19.5±4.9	0.984±0.34
5i	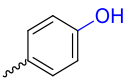	3.82±0.22	**0.180±0.001**

The most significant activities are highlighted in bold

In the cases of **6e** and **6h**, the *S* absolute configuration (the D relative configuration) of the P1 fragment was discriminating for the porcine-originated aminopeptidase. The *S*,*R* and *S*,*S* diastereoisomers interacted poorly in the active site and did not utilize contacts with the catalytic metal cation. By contrast, *Hs*APN was less demanding and accepted distinct forms, e.g., all four stereoisomers of **6e** gave rise to high-energy interactions (Table 2 and Fig. 1). Thus, the highest measured potency of this phosphinic dipeptide could be explained by the Zn-phosphinate coordination, and a range of tight contacts between both the inhibitor backbone and the side chains with the enzyme residues found for each diastereoisomer. The modeled binding mode of stereoisomer ***R*,*S*-6e** (corresponding to the natural L,L configuration) with *Hs*APN revealed the prototypical bidentate coordination of the negatively charged phosphinate moiety to the zinc metal ion (Fig. 1b). In addition, one of the phosphinate oxygen atoms forms a hydrogen bond network with the carboxylate of Glu411 and imidazole nitrogen of His388. Another set of hydrogen bonds involve interactions of the inhibitor amino group with the carboxylate Glu411 and the hydroxylate of Tyr477. The C-terminal functionality has contacts with the guanidine of Arg381 and the N-H of Ala353. The side chains fit well in the spacious and hydrophobic binding pockets as the biphenyl ring has an increased surface area involved in lipophilic interactions with the residues of the S1' cavity, e.g., His388 and Glu418. Quite unexpectedly, its enantiomer (***S*,*R*-6e**, corresponding to D,D relative configuration) was capable of an even more favorable set of polar contacts: (1) > PO^{2-} with Zn^{2+} and with HO– of Tyr477, (2) $–NH_3^+$ with COO^- of Glu355, Glu389 and with C=O of Ala353, and (3) COO– with guanidine of Arg381, accompanied by the penetration of the hydrophobic enzyme pockets with the side-chain residues (Fig. 1c). This complementarity gave rise to an increased free energy of binding.

Although bound to the central metal ion *via* phosphinate, the best poses of the two remaining stereoisomers were somewhat less conveniently accommodated by *Hs*APN and avoided the canonical interaction mode. In fact, the overall arrangements implied the reverse binding of the side-chain residues, namely, the P1 to the S1' pocket and the P1' to the S1 pocket. The bent backbone conformations oriented the polar groups in front of each other on the same side of the molecule. For ***R*,*R*-6e**, the acidic groups, namely, phosphinate and carboxylate, were positioned in parallel and both complexed with Zn^{2+} *via* one oxygen atom (Fig. 1a). The remaining oxygen atoms formed hydrogen bonds with the neighboring residues of Gln213, Ala351 and Glu355. The amino group conserved an opportunity to form only a single electrostatic contact with Glu389. For ***S*,*S*-6e**, the phosphinate interacted in a bidentate manner with the zinc atom, and with the hydroxyl group of Tyr477 (Fig. 1d). The inhibitor carboxylate was positioned in proximity to the amino functionality to form an intramolecular salt bridge that stabilized the overall conformation. The C- and N-termini were also involved in a set of hydrogen bonds with the heteroatoms of Gln211, Glu355 and Met 354. The binding modes of these two stereoisomers were less favorable and characterized by a somewhat higher calculated free energy.

Conclusion

To conclude, we suggested phosphinic dehydrodipeptides as potential inhibitors of metalloaminopeptidases; however, these compounds did not reach the high affinity of their

Table 2 Inhibition of mammalian alanyl aminopeptidases by selected phosphinic dipeptides (**6e** and **6h**) compared to their dehydro analogs (**5e** and **5h**)

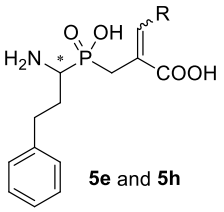

5e and **5h**

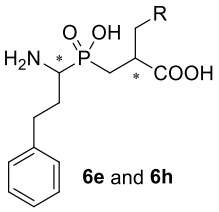

6e and **6h**

Configuration		*R*-(*E*)	*R*-(*Z*)	*S*-(*E*)	*S*-(*Z*)	*R*,*R*	*R*,*S*	*S*,*R*	*S*,*S*
R = 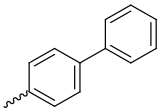									
*Ss*APN	K_i [μM]		0.850±0.060				1.28±0.26		
	ΔG [kcal/mol]	-272	-38.2*	-158	-49.2*	-199	-259	-150*	-258*
*Hs*APN	K_i [μM]		0.151±0.028				0.021±0.011		
	ΔG [kcal/mol]	-297*	-349	-352	-406	-308	-367	-398	-315
R 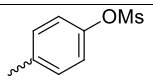									
*Ss*APN	K_i [μM]		19.5±4.9				2.85±0.75		
	ΔG [kcal/mol]	-204	-169	-232	-93.1*	-241	-236	-162*	-120*
*Hs*APN	K_i [μM]		0.984±0.34				0.035±0.0045		
	ΔG [kcal/mol]	-373	-290*	-370	-284*	-210*	-375	-399	-390

The kinetic data are further illustrated by free binding energy values, calculated for the stereo-defined ligand-protein complexes using the GOLD docking protocols with in situ minimization

saturated analogs. Because of structural constraints, the anti-aminopeptidase activity of the double bond-containing compounds appeared to be much more dependent on the configuration of individual stereoisomers and composition of the materials. Certain arrangements of dehydrodipeptides were suggested to lead to weak nonclassical binding that did not implicate coordination with the catalytic metal ion in the active center. To achieve the desired ligand-enzyme complementarity, these compounds must be synthesized in an entirely stereoselective manner. For phosphinic dipeptides, the configuration appeared to be less discriminating. Certain stereoisomers were clearly preferred, in particular by porcine APN, but the rotational freedom gave rise to a lower binding energy of the distinct diastereomeric forms. While the detailed mode of interaction was apparently dependent on the structure of the side-chain substituents, an advantageous fit was found more frequently for the saturated compounds than for their unsaturated counterparts. Thus, to achieve active compounds, the convenient synthetic protocol adopted for phosphinic dehydrodipeptides and based on the substitution of the Morita–Baylis–Hillman acetates with aminoalkylphosphinic acids should be extended by the subsequent reduction. The whole procedure is mild and can be readily performed for different P1' substituents.

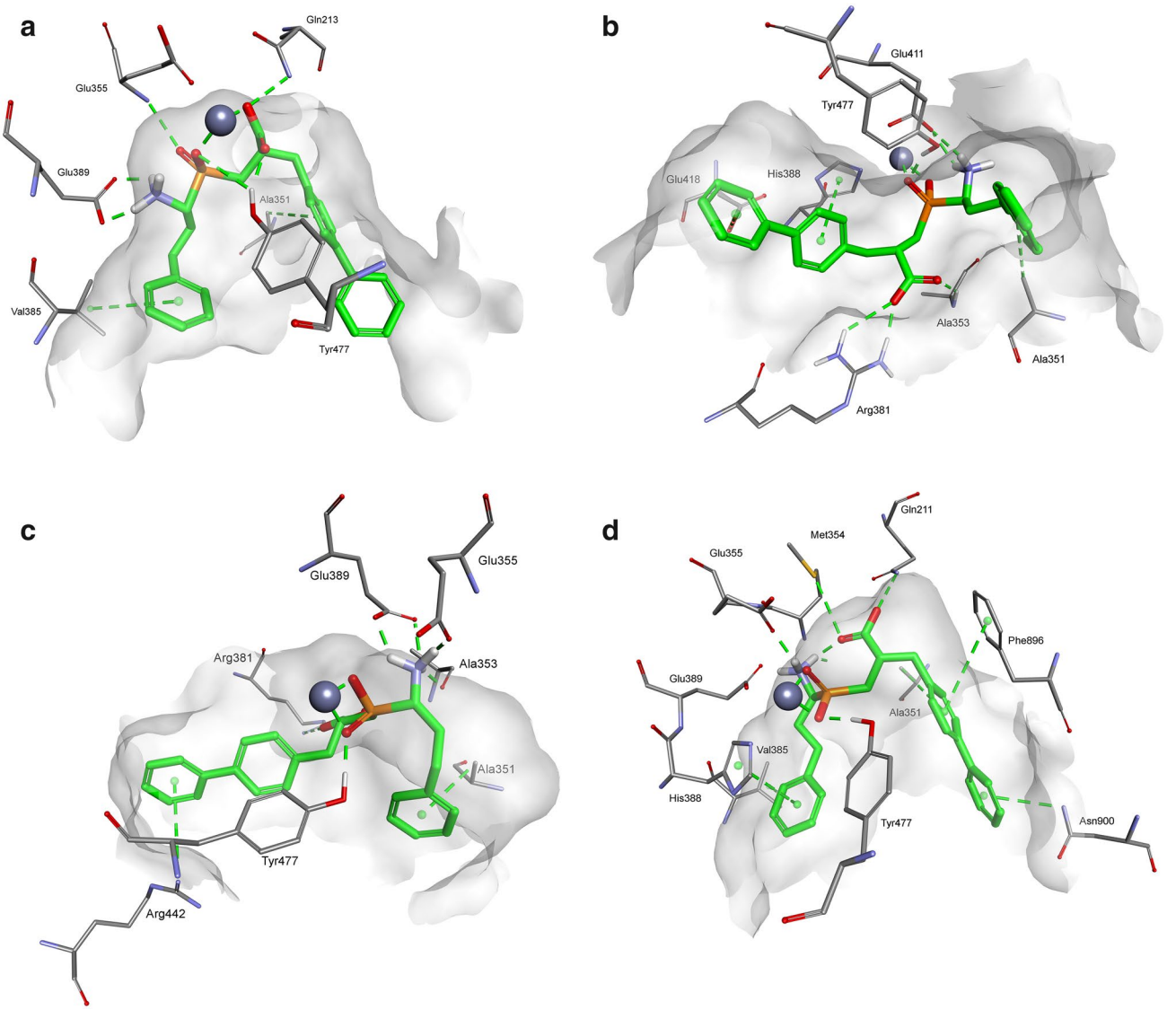

Fig. 1 Modeled binding modes of diastereoisomers of **6e** to *Hs*APN (PDB:4FYT) (Wong et al. 2012): **a** (*R*,*R*), **b** (*R*,*S*), **c** (*S*,*R*), **d** (*S*,*S*). Inhibitors and enzyme amino acid residues are shown as sticks, while the zinc ion is represented by a dark blue sphere. Hydrogen bonds and interactions with metal ions are shown as thin green lines. The surface of the enzyme is shown in gray.

Acknowledgements This work was financed by a grant from the Polish National Science Centre to Artur Mucha (Grant 2013/09/B/ST5/00090). The Biovia Discovery Studio package was used under a Polish country-wide license. The use of the software resources (BIOVIA Discovery Studio program package) of the Wrocław Centre for Networking and Supercomputing is kindly acknowledged.

Compliance with Ethical Standards

Ethical Approval This article does not contain any studies with human participants or animals performed by any of the authors.

Conflict of interest Author declares that he has no conflict of interest.

References

Basavaiah D, Pandiaraju S (1996) Nucleophilic addition of triethyl phosphite to acetates of the Baylis–Hillman adducts: stereoselective synthesis of (E)- and (Z)-allylphosphonates. Tetrahedron 52:2261–2268. https://doi.org/10.1016/0040-4020(95)01055-6

Baylis EK, Campbell CD, Dingwall JG (1984) 1-Aminoalkylphosphonous acids. Part 1. Isosteres of the protein amino acids. J Chem Soc Perkin Trans 1:2845–2853. https://doi.org/10.1039/P19840002845

Boyd EA, Corless M, James K, Regan AC (1990) A versatile route to substituted phosphinic acids. Tetrahedron Lett 31:2933–2936. https://doi.org/10.1016/0040-4039(90)80188-R

Chen H, Noble F, Mothé A, Hervé M, Coric P, Danascimento S, Roques BP, George P, Fournié-Zaluski MC (2000) Phosphinic derivatives as new dual enkephalin-degrading enzyme inhibitors: synthesis, biological properties, and antinociceptive

activities. J Med Chem 43:1398–1408. https://doi.org/10.1021/jm9904831

Chen S, Coward JK (1996) A general method for the synthesis of N-protected α-aminoalkylphosphinic acids. Tetrahedron Lett 37:4335–4338. https://doi.org/10.1016/0040-4039(96)00839-8

Collinsová M, Jirácek J (2000) Phosphinic acid compounds in biochemistry, biology and medicine. Curr Med Chem 7:629–647. https://doi.org/10.2174/0929867003374831

Georgiadis D, Cuniasse P, Cotton J, Yiotakis A, Dive V (2004) Structural determinants of RXPA380, a potent and highly selective inhibitor of the angiotensin-converting enzyme C-domain. Biochemistry 43:8048–8054. https://doi.org/10.1021/bi049504q

Georgiadis D, Dive V (2015) Phosphinic peptides as potent inhibitors of zinc-metalloproteases. Top Curr Chem 360:1–38. https://doi.org/10.1007/128_2014_571

Grembecka J, Mucha A, Cierpicki T, Kafarski P (2003) The most potent organophosphorus inhibitors of leucine aminopeptidase. Structure-based design, chemistry, and activity. J Med Chem 46:2641–2655. https://doi.org/10.1021/jm030795v

Gurulingappa H, Buckhalts P, Kinzler KW, Vogelstein B, Khan SR (2004) Synthesis and evaluation of aminophosphinic acid derivatives as inhibitors of renal dipeptidase. Bioorg Med Chem Lett 14:3531–3533. https://doi.org/10.1016/j.bmcl.2004.04.057

Gurulingappa H, Buckhaults P, Kumar SK, Kinzler KW, Vogelstein B, Khan SR (2003) Design, synthesis and evaluation of new RDP inhibitors. Tetrahedron Lett 44:1871–1873. https://doi.org/10.1016/S0040-4039(03)00082-0

Joshi S, Chen L, Winter MB, Lin YL, Yang Y, Shapovalova M, Smith PM, Liu C, Li F, LeBeau (2017) The rational design of therapeutic peptides for aminopeptidase N using a substrate-based approach. Sci Rep 7:1424–1434. https://doi.org.10.1038/s41598-017-01542-5

Kalyva M, Zografos AL, Kapourani E, Giambazolia E, Devel L, Papakyriakou A, Dive V, Lazarou Y, Georgiadis D (2015) Probing the mechanism of allylic substitution of Morita–Baylis–Hillman acetates (MBHAs) by using the silyl phosphonite paradigm: scope and applications of a versatile transformation. Chem Eur J 21:3278–3289. https://doi.org/10.1002/chem.201405626

Matziari M, Beau F, Cuniasse P, Dive V, Yiotakis A (2004) Evaluation of P1'-diversified phosphinic peptides leads to the development of highly selective inhibitors of MMP-11. J Med Chem 47:325–336. https://doi.org/10.1021/jm0308491

Matziari M, Georgiadis D, Dive V, Yiotakis A (2001) Convenient synthesis and diversification of dehydroalaninyl phosphinic peptide analogues. Org Lett 3:659–662. https://doi.org/10.1021/ol006991 03

Matziari M, Nasopoulou M, Yiotakis A (2006) Active methylene phosphinic peptides: a new diversification approach. Org Lett 8:2317–2319. https://doi.org/10.1021/ol060575m

Morita K, Suzuki Z, Hirose H (1958) A tertiary phosphine-catalyzed reaction of acrylic compounds with aldehydes. Bull Chem Soc Jpn 41:2815–2815. https://doi.org/10.1246/bcsj.41.2815

Mucha A (2012) Synthesis and modifications of phosphinic dipeptide analogues. Molecules 17:13530–13568. https://doi.org/10.3390/molecules171113530

Mucha A, Kafarski P, Berlicki Ł (2011) Remarkable potential of the α-aminophosphonate/ phosphinate structural motif in medicinal chemistry. J Med Chem 54:5955–5980. https://doi.org/10.1021/jm200587f

Ohgiya T, Nishiyama S (2004) A simple deprotection of triflate esters of phenol derivatives. Tetrahedron Lett 45:6317–6320. https://doi.org/10.1016/j.tetlet.2004.06.104

Parsons WH, Hajdu R, Schoen WR, Combs PL, Sundelof J, Patchett AA (1991) A new class of potent, slowly reversible dehydropeptidase inhibitors. Biochem Int 23:1107–1115

Parsons WH, Patchett AA, Bull HG, Schoen WR, Taub D, Davidson C, Combs P, Springer JP, Gadebusch H, Weissberger B, Valiant ME, Mellin TN, Busch RD (1988) Phosphinic acid inhibitors of D-alanyl-D-alanine ligase. J Med Chem 31:1772–1778. https://doi.org/10.1021/jm00117a017

Skinner-Adams TS, Stack CM, Trenholme KR, Brown CL, Grembecka J, Lowther J, Mucha A, Drag M, Kafarski P, McGowan S, Whisstock JC, Gardiner DL, Dalton JP (2010) *Plasmodium falciparum* neutral aminopeptidases: new targets for anti-malarials. Trends Biochem Sci 35:53–61. https://doi.org/10.1016/j.tibs.2009.08.004

Stetter H, Kuhlmann H (1979) Eine einfache herstellung von α-alkylacrylsäure-estern. Synthesis 1979:29–30. https://doi.org/10.1055/s-1979-28537

Suzuki K, Muto Y, Fushihara K, Kanemoto K, Iida H, Sato E, Kikuchi C, Matsushima T, Kato E, Nomoto M, Yoshioka S, Ishii H (2004) Enhancement of fibrinolysis by EF6265 [(S)-7-amino-2-[[[(R)-2-methyl-1-(3-phenylpropanoylamino)propyl]hydroxyphosphinoyl]methyl]heptanoic acid], a specific inhibitor of plasma carboxypeptidase B. J Pharmacol Exp Ther 309:607–615. https://doi.org/10.1124/jpet.103.062729

Talma M, Mucha A (2017) P-C bond formation in reactions of Morita-Baylis-Hillman adducts with phosphorus nucleophiles. Arkivoc 324–344. https://doi.org/10.3998/ark.5550190.p009.787

Thottathil JK, Ryono DE, Przybyla CA, Moniot JL, Neubeck R (1984) Preparation of phosphinic acids: Michael additions of phosphonous acids/esters to conjugated systems. Tetrahedron Lett 25:4741–4744. https://doi.org/10.1016/S0040-4039(01)81507-0

Vassiliou S, Mucha A, Cuniasse P, Georgiadis D, Lucet-Levannier K, Beau F, Kannan R, Murphy G, Knauper V, Rio M-C, Basset P, Yiotakis A, Dive V (1999) Phosphinic pseudo-tripeptides as potent inhibitors of matrix metalloproteinases: a structure—activity study. J Med Chem 42:2610–2620. https://doi.org/10.1021/jm9900164

Vassiliou S, Węglarz-Tomczak E, Berlicki Ł, Pawełczak M, Nocek B, Mulligan R, Joachimiak A, Mucha A (2014) Structure-guided, single-point modifications in the phosphinic dipeptide structure yield highly potent and selective inhibitors of neutral aminopeptidases. J Med Chem 57:8140–8151. https://doi.org/10.1021/jm501071f

Wang YX, Zhao L, Nagashima M, Vincelette J, Sukovich D, Li W, Subramanyam B, Yuan S, Emayan K, Islam I, hrvatin P, Bryant J, Light DR, Vergona R, Morser J, Buckman BO (2007) A novel inhibitor of activated thrombin-activatable fibrinolysis inhibitor (TAFIa)—part I: pharmacological characterization. Thromb Haemost 97:45–53. https://doi.org/10.1160/TH06-09-0551

Wong AHM, Zhou D, Rini JM (2012) The X-ray crystal structure of human aminopeptidase N reveals a novel dimer and the basis for peptide processing. J Biol Chem 287:36804–36813. https://doi.org/10.1074/jbc.M112.398842

Yamagishi T, Tashiro N, Yokomatsu T (2011) Diastereoselective synthesis of the Leu-Pro type phosphinyl dipeptide isostere. J Org Chem 76:5472–5476. https://doi.org/10.1021/jo200669r

Yiotakis A, Georgiadis D, Matziari M, Makaritis A, Dive V (2004) Phosphinic peptides: synthetic approaches and biochemical evaluation as Zn-metalloprotease inhibitors. Curr Org Chem 8:1135–1158. https://doi.org/10.2174/1385272043370177

Yu C, Liu B, Hu L (2001) Efficient Baylis–Hillman reaction using stoichiometric base catalyst and an aqueous medium. J Org Chem 66:5413–5418. https://doi.org/10.1021/jo015628m